

The Frequency Structure of 1D Occluding Image Signals

Steven S. Beauchemin and John L. Barron

Abstract— We present a theoretical investigation of the frequency structure of 1D occluding image signals. We show that image signal occlusion contains relevant information which is most easily extractable from its representation in the frequency domain. For instance, the occluding and occluded signal velocities may be identified as such and translucency phenomena may be understood in the terms of this theoretical investigation. In addition, it is found that the structure of occluding 1D signals is invariant under constant and linear models of signal velocity. This theoretical framework can be used to describe the exact frequency structure of non-Fourier motion and bridges the gap between such visual phenomena and their understanding in the frequency domain.

Keywords— Occlusion, Fourier transforms, Optical Flow, Non-Fourier motion

I. INTRODUCTION

THE problem posed by occlusion and translucency phenomena is investigated for 1D image signals. Traditionally, signal velocity has been computed directly from spatial extents with tracking and matching processes or spatiotemporal derivatives. These techniques impose stringent signal characteristics to ensure their correctness. For instance, spatiotemporal numerical derivation of a translating signal implies the sampling of a continuous signal over the extent of derivation. Such processes approximate reality only if computed over extents that do not contain occlusion discontinuities or that are not a mixture of two or more signals due to translucent effects.

The inability of classical spatiotemporal processes to resolve signal velocity over extents exhibiting signal occlusion or translucency indicates that such phenomena might be better understood in another domain of representation. We postulate that spatiotemporal information constitutes an obstacle to determining the translational rates of occluding or translucent 1D image signals and we derive, for various models of translation and in the frequency domain, several theorems describing the frequency structure of signal discontinuities arising from occlusion in the spatiotemporal domain. We consider constant and linear models of signal translation and show that translucency phenomena may be understood as special cases of the theoretical results exposed herein.

Steven S. Beauchemin is with the GRASP Laboratory, University of Pennsylvania, 3401 Walnut Street, Suite 300C, Philadelphia, PA, 19104-6228. E-mail: beau@grip.cis.upenn.edu

John L. Barron is an Associate Professor of Computer Science at The University of Western Ontario, London, Canada, N6A 5B7. E-mail: barron@csd.uwo.ca

A. Methodology

To analyze the frequency structure of 1D occluding image signals while preserving representations that are as general as possible, an effort is made to pose only those hypotheses that preserve the generality of the analysis to follow. We describe the assumptions and the proof techniques with which the theoretical results are obtained.

Image Signals The geometry of image formation, although a simple process, generally yields complex signals. Conceptually, assumptions concerning scene structure should not be made, as they constrain the geometry of observable scenes. In addition, any measured physical signal, such as image intensities, satisfies Dirichlet conditions. Such signals admit a finite number of finite discontinuities, are absolutely integrable and may be expanded into complex exponential series. Dirichlet conditions constitute the sum of assumptions made on 1D image signals.

Velocity On a local basis, constant models of signal translation may be adequate to describe velocity. However, linear models admit an increased number of deformations, such as signal dilation. Hence, the extent used for signal analysis may be larger with linear models. We considered both constant and linear models, leaving deformations of higher order for further analysis.

Occluding Points Occluding points in 1D image signals are represented with Heaviside's functions. In 1D, this model is adequate in the sense that it entirely comprises the occluding phenomenon. However, when 2D signals are concerned, occluding boundaries between objects and backgrounds may have various shapes and the use of a 2D Heaviside's function as an occluding boundary model limits the validity of the analysis to local extents.

Proof Techniques The Theorems and their Corollaries established in this analysis emanate from a general approach to modeling 1D signals exhibiting occlusion discontinuities. An equation which describes the spatiotemporal pattern of the superposition of a 1D background and an occluding 1D signal is given [3].

A characteristic function describing the position an occluding signal occupies within the imaging space of the visual sensor is defined as

$$\chi(x) = \begin{cases} 1 & \text{if } x \text{ within extent of occluding signal} \\ 0 & \text{otherwise,} \end{cases} \quad (1)$$

and two 1D image signals $\mathbf{I}_1(x)$ and $\mathbf{I}_2(x)$, corresponding to the occluding and occluded signals respectively,

are defined to form the complete signal pattern

$$\begin{aligned} \mathbf{I}(x, t) &= \mathbf{I}_1(v_1^{(n)}(x, t))\chi(v_1^{(n)}(x, t)) \\ &+ \left[1 - \chi(v_1^{(n)}(x, t))\right] \mathbf{I}_2(v_2^{(n)}(x, t)), \end{aligned} \quad (2)$$

where n in $v_i^{(n)}(x, t)$ represents the model of velocity being used. For instance, $n = 0$ is constant and $n = 1$ is linear velocity. Note that the characteristic function describing the object in (2) has the same velocity as its corresponding intensity pattern $\mathbf{I}_1(x)$.

In this equation are inserted the hypotheses made on its various components and the structure of 1D occlusion in the frequency domain is developed. That is to say, signal structures are expanded into complex exponential series

$$\mathbf{I}_i(x) = \sum_{n=-\infty}^{\infty} c_{in} e^{ixnk_i}, \quad (3)$$

where $\mathbf{I}_i(x)$ is the i^{th} intensity pattern, c_{in} are complex coefficients, n are integers, and k_i is the fundamental frequency of the expansion. This frequency represents the discretization step of the signal. Occlusion boundaries are represented with 1D Heaviside's functions

$$\mathbf{u}(x) = \begin{cases} 1 & \text{if } x \geq 0 \\ 0 & \text{otherwise.} \end{cases} \quad (4)$$

Relevance of Fourier Analysis Many algorithms operating in the Fourier domain for which a claim of multiple motions capability is made have been developed [7]. However, this is performed without a complete knowledge of the frequency structure of occlusion phenomena. In addition, non-Fourier spectra, including occlusion and translucency effects have been conjectured to have mathematically simple characterizations in Fourier space [5]. Consequently, the use of Fourier analysis as a local tool is justified as long as one realizes that it constitutes a global idealization of local phenomena. In that sense, Fourier analysis is used as a local tool whenever Gabor filters, wavelets or local Discrete Fourier Transforms are employed for signal analysis.

Experimental Technique Given the theoretical nature of this contribution, the purpose of the numerical experiments is to verify the validity of the theoretical results. In order to accomplish this, the frequency content of the image signals used in the experiments must be entirely known to the experimenter, thus forbidding the use of natural image sequences. In addition, image signals with single frequency components are used in order to facilitate the interpretation of experiments involving Fast Fourier transforms. The use of more complex signals impedes a careful examination of the numerical results and do not extend the understanding of the phenomena under study in any particular way.

B. Problem Definition

It is clear that velocity discontinuities are different from signal discontinuities. However, there is a recurrent confusion within the existing literature related to optical flow. For instance, many image velocity techniques which employ regularization processes often include a relaxation of the smoothness requirement within extents exhibiting strong intensity variations [8], [9], [10], [1], although signal discontinuities may not correspond to velocity discontinuities. Indeed, the discontinuities caused by occlusion are extrinsic whereas signal discontinuities are intrinsic in terms of signal properties.

II. OCCLUSION IN THE FREQUENCY DOMAIN

The Fourier transform of a translating 1D image signal $\mathbf{I}(x, t)$ is obtained with the shift property as

$$\begin{aligned} \hat{\mathbf{I}}(k, \omega) &= \int \int \mathbf{I}(x - vt) e^{-i(kx + \omega t)} dx dt \\ &= \hat{\mathbf{I}}(k) \delta(kv + \omega), \end{aligned} \quad (5)$$

where $kv + \omega = 0$ represents an oriented line containing the origin of the frequency domain, onto which the spectrum $\hat{\mathbf{I}}(k)$ lies. The slope of the linear spectrum is proportional to v , the velocity of the signal.

Following Fleet and Jepson [4], velocity discontinuities arising from occlusion may be written by considering two translating signals, one partially occluding the other. Let $\mathbf{I}_1(x)$ and $\mathbf{I}_2(x)$ be two translating signals coupled with the characteristic function (1) indicating the occluding signal position. The resulting 1D occlusion scene may be written in terms of the translating signals and the characteristic function as

$$\begin{aligned} \mathbf{I}(x, t) &= \mathbf{I}_1(x - v_1 t) \chi(x - v_1 t) \\ &+ [1 - \chi(x - v_1 t)] \mathbf{I}_2(x - v_2 t). \end{aligned} \quad (6)$$

By using the shift property of Fourier transforms, (6) is rewritten in spatiotemporal frequency space as

$$\begin{aligned} \hat{\mathbf{I}}(k, \omega) &= [\hat{\mathbf{I}}_1(k) \delta(kv_1 + \omega)] * [\hat{\chi}(k) \delta(kv_1 + \omega)] \\ &- [\hat{\mathbf{I}}_2(k) \delta(kv_2 + \omega)] * [\hat{\chi}(k) \delta(kv_1 + \omega)] \\ &+ \hat{\mathbf{I}}_2(k) \delta(kv_2 + \omega). \end{aligned} \quad (7)$$

The first two terms of (7) correspond to the occluding and occluded signals convolved with the Fourier spectrum of the occlusion boundary and constitute the spectral distortion introduced by the discontinuity.

A. Models of Velocity

The velocity function may be expressed as a polynomial in the coordinate system of the signal. Generally, a Taylor series expansion for an i^{th} image plane velocity may be written as

$$v_i(x, t) = \sum_{j=0}^p \sum_{k=0}^q \frac{\partial^{j+k} v_i}{j! k! \partial x^j \partial t^k} x^j t^k \Big|_{x, t = \vec{0}} \quad (8)$$

where $p + q \leq n$. We adopt the notation $v_i^{(1)}(x, t) = a_{i1}x - a_{i2}t$ to describe 1D, linear velocity and $v_i^{(0)}(x, t) = x - a_{i2}t$ for constant velocity. Negative rates of translation are used without loss of generality and for mere mathematical convenience.

B. Occlusion with Constant Velocity

In this section, two cases of occlusion with constant models of velocity are considered. The analysis begins with the consideration of a simple case consisting of 1D sinusoidal intensity profiles translating at constant velocities. This result is then generalized to arbitrary signals and linear models of velocity.

B.1 Sinusoidal Signals

Let $\mathbf{I}_1(x)$ be occluding a 1D intensity pattern $\mathbf{I}_2(x)$, with respective velocities $v_1^{(0)}(x, t)$ and $v_2^{(0)}(x, t)$. The resulting intensity profile can then be expressed as

$$\begin{aligned} \mathbf{I}(x, t) &= \mathbf{u}(v_1^{(0)}(x, t))\mathbf{I}_1(v_1^{(0)}(x, t)) \\ &+ (1 - \mathbf{u}(v_1^{(0)}(x, t)))\mathbf{I}_2(v_2^{(0)}(x, t)) \end{aligned} \quad (9)$$

where $\mathbf{u}(x)$ is (4). The Fourier transform of (9) is

$$\begin{aligned} \hat{\mathbf{I}}(k, \omega) &= [\hat{\mathbf{u}}(k)\delta(ka_{12} + \omega)] * [\hat{\mathbf{I}}_1(k)\delta(ka_{12} + \omega)] \\ &- [\hat{\mathbf{u}}(k)\delta(ka_{12} + \omega)] * [\hat{\mathbf{I}}_2(k)\delta(ka_{22} + \omega)] \\ &+ \hat{\mathbf{I}}_2(k)\delta(ka_{22} + \omega), \end{aligned} \quad (10)$$

where $\hat{\mathbf{u}}(k) = \pi\delta(k) + (ik)^{-1}$ is the Fourier transform of Heaviside's function.

Theorem 1: Let $\mathbf{I}_1(x)$ and $\mathbf{I}_2(x)$ be cosine functions with respective angular frequencies $k_1 = 2\pi f_1 > 0$ and $k_2 = 2\pi f_2 > 0$ and let $\mathbf{I}_1(v_1^{(0)}(x, t)) = c_1 \cos(k_1(x - a_{12}t))$ and $\mathbf{I}_2(v_2^{(0)}(x, t)) = c_2 \cos(k_2(x - a_{22}t))$. The frequency spectrum of the occlusion is

$$\begin{aligned} \hat{\mathbf{I}}(k, \omega) &= \frac{\pi}{2}c_1\delta(k \pm k_1, \omega \mp k_1a_{12}) + \\ &\frac{(1 - \pi)}{2}c_2\delta(k \pm k_2, \omega \mp k_2a_{22}) + \\ &\frac{i}{2} \left(\frac{c_2\delta(ka_{12} + \omega \pm k_2\Delta a_2)}{(k \pm k_2)} - \frac{c_1\delta(ka_{12} + \omega)}{(k \pm k_1)} \right) \end{aligned} \quad (11)$$

where $\Delta a_2 = a_{12} - a_{22}$.

Theorem 1 is derived to characterize occlusion with the simplest parameters, such as a constant model of velocity, the structure of occlusion boundaries and the number of distinct frequencies to represent both the occluding and occluded signals. A number of fundamental observations can still be made even under these restrictive assumptions:

- The occlusion scene in frequency space consists of the Fourier transform of Heaviside's function convolved with every non-zero frequencies of both the occluding and occluded signals. The result of these convolutions

are the distortion terms cast by the phenomenon of occlusion.

- The power content of the distortion term forms linear spectra of decreasing power about the frequencies of both signals and their orientation is consonant with the velocity of the occluding signal. Hence, The detection of this orientation allows to identify the occluding velocity, leaving the occluded velocity to be interpreted as such.

B.2 Generalized Signals

In general, the occluding and occluded signals cannot be represented as simple sinusoidal functions. To gain generality, $\mathbf{I}_1(x)$ and $\mathbf{I}_2(x)$ are expanded as complex exponential expansions, assuming that functions $\mathbf{I}_1(x)$ and $\mathbf{I}_2(x)$ satisfy Dirichlet conditions [6].

Theorem 2: Let $\mathbf{I}_1(x)$ and $\mathbf{I}_2(x)$ be functions satisfying Dirichlet conditions such that they may be expressed as complex exponential series expansions

$$\begin{aligned} \mathbf{I}_1(x) &= \sum_{n=-\infty}^{\infty} c_{1n}e^{ink_1x} \\ \mathbf{I}_2(x) &= \sum_{n=-\infty}^{\infty} c_{2n}e^{ink_2x}, \end{aligned} \quad (12)$$

where n is integer, c_{1n} and c_{2n} are complex coefficients and k_1 and k_2 are the fundamental frequencies of the expansions. Let $\mathbf{I}_1(x, t) = \mathbf{I}_1(v_1^{(0)}(x, t))$ and $\mathbf{I}_2(x, t) = \mathbf{I}_2(v_2^{(0)}(x, t))$. The frequency spectrum of the occlusion is

$$\begin{aligned} \hat{\mathbf{I}}(k, \omega) &= \pi \sum_{n=-\infty}^{\infty} c_{1n}\delta(k - nk_1, \omega + nk_1a_{12}) \\ &+ (1 - \pi) \sum_{n=-\infty}^{\infty} c_{2n}\delta(k - nk_2, \omega + nk_2a_{22}) \\ &+ i \sum_{n=-\infty}^{\infty} \left(\frac{c_{2n}\delta(ka_{12} + \omega - nk_2\Delta a_2)}{(k - nk_2)} \right. \\ &\quad \left. - \frac{c_{1n}\delta(ka_{12} + \omega)}{(k - nk_1)} \right). \end{aligned} \quad (13)$$

Theorem 2 generalizes Theorem 1 to signals composed of an arbitrary number of discrete frequencies. Dirichlet conditions are hypothesized for each signal, since any physical signal satisfies such conditions. The properties of Theorem 1 hold for the generalized signals of Theorem 2. Indeed, both velocities and their respective signals can be discriminated, as is the case for Theorem 1.

The definition of signal velocity as a constant translational rate is limited. To gain generality, signal dilation is included and the velocity function is written as $v_i^{(1)}(x, t) = a_{i1}x - a_{i2}t$.

Theorem 3: Let $\mathbf{I}_1(a_{11}x)$ and $\mathbf{I}_2(a_{21}x)$ be functions satisfying Dirichlet conditions such that they may be expressed as complex exponential series expansions:

$$\mathbf{I}_1(a_{11}x) = \sum_{n=-\infty}^{\infty} c_{1n}e^{ink_1a_{11}x}$$

$$\mathbf{I}_2(a_{21}x) = \sum_{n=-\infty}^{\infty} c_{2n} e^{ink_2 a_{21}x}, \quad (14)$$

where n is integer, c_{1n} and c_{2n} are complex coefficients and k_1 and k_2 are the fundamental frequencies of the expansions. Also let $\mathbf{I}_1(x, t) = \mathbf{I}_1(v_1^{(1)}(x, t))$ and $\mathbf{I}_2(x, t) = \mathbf{I}_2(v_2^{(1)}(x, t))$. The frequency spectrum of occlusion is

$$\begin{aligned} \hat{\mathbf{I}}(k, \omega) &= \pi \sum_{n=-\infty}^{\infty} c_{1n} \delta(k - nk_1 a_{11}, \omega + nk_1 a_{12}) \\ &+ (1 - \pi) \sum_{n=-\infty}^{\infty} c_{2n} \delta(k - nk_2 a_{21}, \omega + nk_2 a_{22}) \\ &+ i \operatorname{sgn}(a_{11}) \sum_{n=-\infty}^{\infty} \left(\frac{c_{2n} \delta(\psi_1 k + \omega - nk_2 \phi_{12})}{(k - nk_2 a_{21})} \right. \\ &\quad \left. - \frac{c_{1n} \delta(\psi_1 k + \omega)}{(k - nk_1 a_{11})} \right) \end{aligned} \quad (15)$$

where

$$\psi_i = \frac{a_{i2}}{a_{i1}} \quad \text{and} \quad \phi_{ij} = \frac{a_{j1} a_{i2} - a_{i1} a_{j2}}{a_{i1}}$$

Theorem 3 shows the frequency structure of occluding 1D image signals and, when put in relation with Theorem 2, it is observed that the structure of occlusion is invariant with respect to both constant and linear models of velocity.

Theorems 1 through 3 show the structure of occlusion in the Fourier domain for constant and linear models of velocity for 1D image signals. These structures have interesting properties which we proceed to formally state in the form of Corollaries.

Corollary 1: The structure of occlusion is invariant under constant and linear models of velocity.

Under constant and linear models of velocity, it is found that the structural aspect of the Fourier spectrum is identical. The power generated by the distortion fits lines that are parallel to the constraint line of the occluding signal. Although the orientation of these structures depict ratios of the linear parameters, a collection of those in a spatiotemporal extent yields these parameters in the least-squares sense. This result also indicates that this structural invariance may be used to detect occlusions under constant or linear velocity equally accurately with a unique mechanism.

Corollary 2: Under an occlusion phenomenon, the velocities of the occluding and occluded signals can always be identified as such.

Under occlusion, the orientations of the distortion terms are essentially parallel to the constraint line of the occluding signal. Hence, the orientation of the constraint line containing the origin and parallel to the distortion terms yields the velocity of the occluding signal, thus leaving the occluded signal velocity to be interpreted as such.

B.3 Geometric Interpretation

We performed a series of experiments to graphically demonstrate the composition of a simple occlusion scene composed of 1D sinusoidal signals. In addition, the signals

are Gaussian-windowed to avoid the Gibbs phenomenon when computing their Fast Fourier Transforms (FFTs). Figure 1a, b and c show the components of a simple occlusion scene, pictured in Figure 1d. Figure 1a is the occluding signal with spatial frequency $\frac{2\pi}{16}$ and velocity -1.0 , such that

$$\mathbf{I}_1(x, t) = \cos\left(\frac{2\pi}{16}(x + t)\right) \quad (16)$$

and in 1b) is the occluded signal with spatial frequency $\frac{2\pi}{8}$ and velocity 1.0, yielding

$$\mathbf{I}_2(x, t) = \cos\left(\frac{2\pi}{8}(x - t)\right). \quad (17)$$

The occluding boundary in Figure 1c) is the 1D step function (4) and translates with a velocity identical to that of the occluding signal.

The resulting occlusion scene in Figure 1d) is constructed with (6), where \mathbf{I}_1 is (16), \mathbf{I}_2 is (17) and χ is (4). Figures 1e through h show the amplitude spectra of figures 1a through d) respectively, where it is easily observed the spectrum of the step function (4) is convolved with each frequency of both sinusoids.

III. NUMERICAL EXPERIMENTS

Several experiments were performed in support of the Theorems. The Fourier spectra obtained with both a standard FFT algorithm and those predicted by the theory are compared. In addition, phase shifts and non-Fourier motions are examined.

In order to perform the numerical experiments, two 1D sinusoids which respectively act as occluding and occluded signals are used.

Expression (9) is used with $\mathbf{I}_1(v_1^{(0)}(x, t)) = c_1 \cos(k_1(x - a_{12}t))$ and $\mathbf{I}_2(v_2^{(0)}(x, t)) = c_2 \cos(k_2(x - a_{22}t))$, where \mathbf{I}_1 and \mathbf{I}_2 are the occluding and occluded signals with respective frequencies $k_1 = \frac{2\pi}{16}$ and $k_2 = \frac{2\pi}{8}$. Constants c_1 and c_2 correspond to signal amplitudes. To limit boundary conditions when numerically computing Fourier transforms, the signal is windowed with a Gaussian envelope. The resulting signal is analytically expressed as

$$\mathbf{I}(x, t)G(x, t; \sigma), \quad (18)$$

where

$$G(x, t; \sigma) = \frac{1}{2\pi\sigma^2} e^{-\left(\frac{x^2 + y^2}{2\sigma^2}\right)}.$$

A standard deviation of 35.0, measured in image units, is used for the windowing of the signal. The discrete Fourier transforms occlusion scenes such as (18) obtained with a standard FFT algorithm are shown in Figure 2e through h. Analytically, the continuous Fourier transform of (18) is

$$\hat{\mathbf{I}}(k, \omega) * \hat{G}(k, \omega; \sigma), \quad (19)$$

where $\hat{\mathbf{I}}(k, \omega)$ is a discretized version of Theorem 1 which models aliasing effects due to periodicity. Figures 2i through l show the corresponding theoretical predictions.

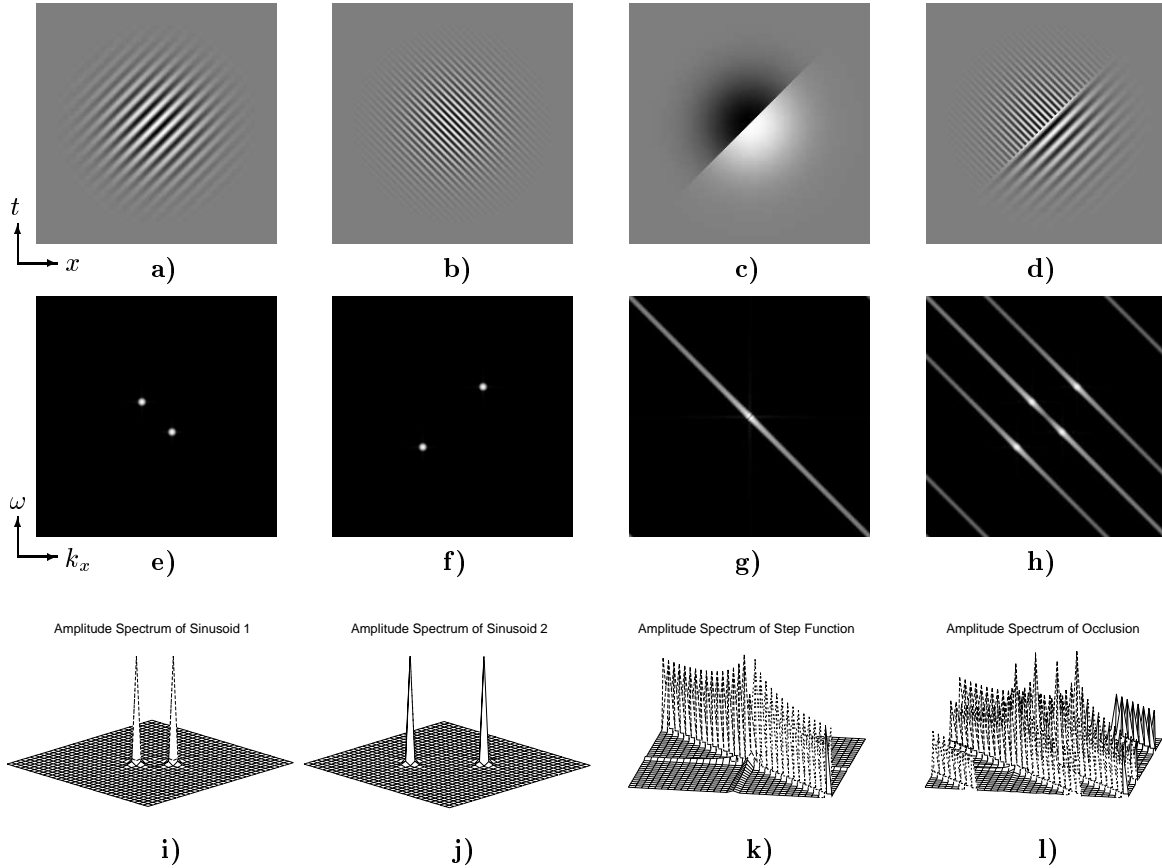


Fig. 1. **(top)**: The composition of a simple 1D occlusion scene. **a)** The occluding sinusoidal signal with frequency $k_1 = \frac{2\pi}{16}$ and velocity $a_{12} = -1.0$. **b)** The occluded sinusoidal signal with frequency $k_2 = \frac{2\pi}{8}$ and velocity $a_{22} = 1.0$. **c)** The translating step function used to create the occlusion scene. **d)** The occlusion as a combination of **a)**, **b)** and **c)**. **(center)**: Image plots of amplitude spectra and **(bottom)**: amplitude spectra as 3D graphs.

The spectra obtained with both a standard FFT algorithm and the theoretical results are essentially identical. These experiments are performed with various velocities for the occluding signal. Figures 2a through d show the occlusion scenes with respective occluding velocities of $a_{11} = -1.0, -0.5, 0.5$ and 1.0 . When both the occluding and occluded signals have identical velocities as in Figure 2d, the spatiotemporal frequencies and the distortion terms align to form a linear spectrum. This is a typical case of signal discontinuities that do not constitute velocity discontinuities. Figure 2 shows that the orientation of the distortion entirely depends on the velocity of the occluding signal. In all cases, the distortion is parallel to the constraint line of the occluding signal.

A. Translucency

In the context of image signals, transmission of light through translucent material may cause multiple signal velocities to arise in a given spatial extent. Generally, this effect is mathematically expressed as

$$\mathbf{I}(x, t) = f(\rho_1)(v_1(x, t))\mathbf{I}_2(v_2(x, t)), \quad (20)$$

where $f(\rho_1)$ is a function of the density of the translucent signal [3]. Under the local assumption of spatially constant $f(\rho_1)$ with translucency factor φ , (20) is reformulated as a weighted superposition of signals, written as

$$\mathbf{I}(x, t) = \varphi\mathbf{I}_1(v_1(x, t)) + (1 - \varphi)\mathbf{I}_2(v_2(x, t)), \quad (21)$$

where $\mathbf{I}_1(v_1(x, t))$ is the intensity profile of the translucent signal and $\mathbf{I}_2(v_2(x, t))$ is the intensity profile of the occluded signal. With $\mathbf{I}_1(v_1(x, t))$ and $\mathbf{I}_2(v_2(x, t))$ satisfying Dirichlet conditions, the frequency spectrum of (21) is written as

$$\begin{aligned} \hat{\mathbf{I}}(k, \omega) &= \varphi \sum_{n=-\infty}^{\infty} c_{1n} \delta(k - nk_1, \omega + nk_1 a_{12}) \\ &+ (1 - \varphi) \sum_{n=-\infty}^{\infty} c_{2n} \delta(k - nk_2, \omega + nk_2 a_{22}) \end{aligned} \quad (22)$$

With the exception of the distortion term, and to within scaling factors, (22) is identical to (15) and, with respect to its frequency structure, translucency may be reduced to a special case of occlusion for which the distortion terms vanish.

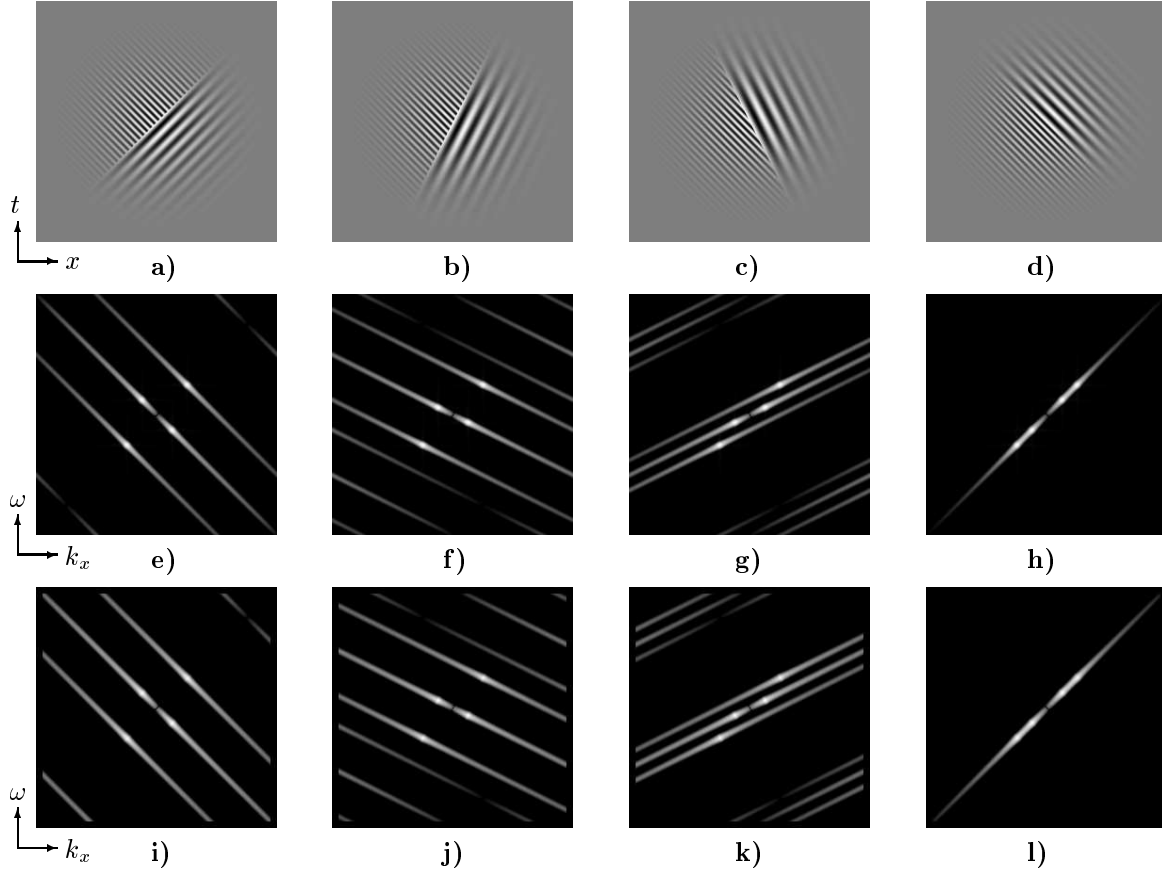


Fig. 2. Comparison of numerical results against theoretical predictions. Frequencies k_1 and k_2 of the occluding and occluded signals are $\frac{2\pi}{16}$ and $\frac{2\pi}{8}$ respectively. The velocity of the occluded signal is $a_{22} = 1.0$. **(top): a)** $a_{12} = -1.0$; **b)** $a_{12} = -0.5$; **c)** $a_{12} = 0.5$; **d)** $a_{12} = 1.0$. **(center): e)** through **h)** Fast Fourier transforms of corresponding occlusion scene **(bottom): i)** through **l)** Theoretical results.

B. Generalized Occluding Point

For reasons of simplicity and clarity, in each Theorem and numerical result, the occluding point contained the origin of the coordinate system. We generalize this by describing the occlusion as

$$\mathbf{u}(x) = \begin{cases} 1 & \text{if } x + t_0 \geq 0 \\ 0 & \text{otherwise} \end{cases}, \quad (23)$$

where t_0 is a shift from the origin and its Fourier spectrum becomes

$$e^{it_0k} (\pi\delta(k) - ik^{-1}) \delta(ka_{i2} + \omega) \quad (24)$$

Equation (23) can be further simplified as

$$\pi\delta(k) - ik^{-1}e^{it_0k}\delta(ka_{i2} + \omega) \quad (25)$$

The Fourier spectrum of the occluding point is to be convolved with the complex exponential series expansions of the occluding and occluded signals and subsequently with the Fourier transform of the Gaussian window. In the case of the occluding signal, the convolution with the the occluding point can be written as

$$\pi \sum_{n=-\infty}^{\infty} c_{1n} \delta(k - nk_1, \omega + nk_1 a_{12}) -$$

$$i e^{it_0(k-nk_1)} \frac{c_{1n} \delta(k - nk_1, ka_{12} + \omega)}{(k - nk_1)} \quad (26)$$

and, similarly for the occluded signal

$$\pi \sum_{n=-\infty}^{\infty} c_{2n} \delta(k - nk_2, \omega + nk_2 a_{22}) - i e^{it_0(k-nk_2)} \frac{c_{2n} \delta(k - nk_2, ka_{22} + \omega)}{(k - nk_2)} \quad (27)$$

These convolutions are combined together to obtain the Fourier spectrum of occlusion with a generalized occluding point. We conducted experiments with 1D image signals and shifted the occlusion point with different values of t_0 in (23). As observed in Figure 3, these phase shifts have no effect on the amplitude spectrum of occlusion in frequency space. The variations in the amplitude spectra are due to the Gaussian windowing of the occlusion scene. For instance, the frequency peaks of the occluding signal in Figure 3e show more power than those of the occluded signal, owing to the fact that the signal is dominant within the Gaussian window. The contrary is observed when the occluded signal occupies most of the window, as shown in Figure 3h.

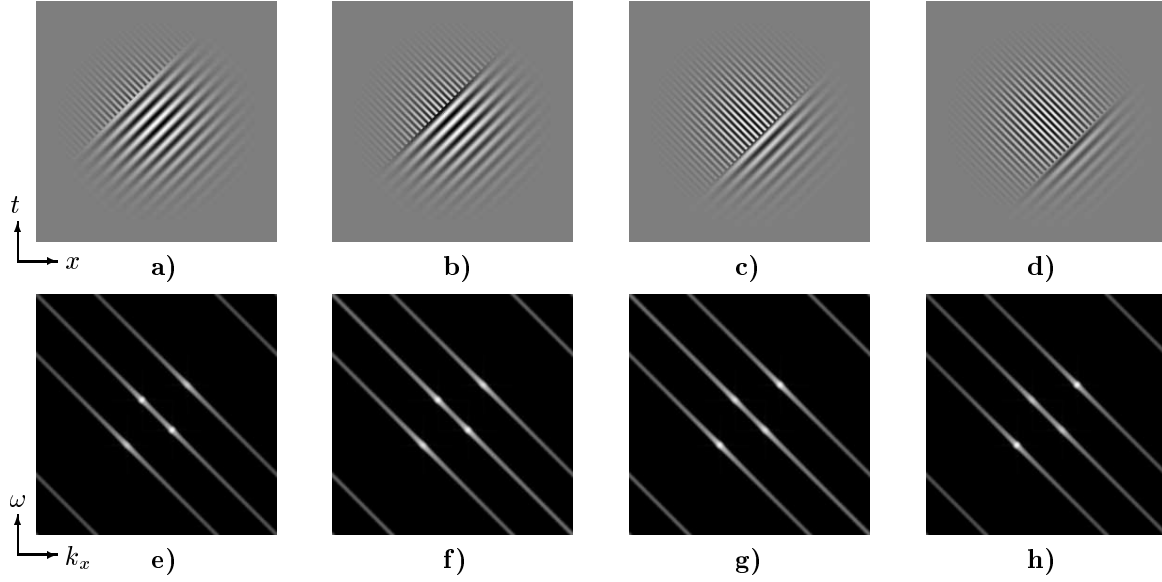


Fig. 3. *Phase shifts from occluding edge. (top): a) $t_0 = -20.0$. b) $t_0 = -10.0$. c) $t_0 = 10.0$. d) $t_0 = 20.0$. (bottom) e) through h): Corresponding frequency spectra. The relative magnitude between the occluding and occluded signals depend on their respective visible areas under the Gaussian envelope. For instance, The frequencies of the occluding signal dominate over those of the occluded signal in e), and vice versa in h).*

C. Non-Fourier Motion

Non-Fourier visual stimuli, to which belong occlusion translucency and occlusion effects, have been studied mainly with respect to the motion percept these stimuli elicit among human subjects [2], [11], [12]. However, more recently, it has been conjectured that a viable computational analysis of Non-Fourier motion could be carried out with Fourier analysis, since many Non-Fourier stimuli appear to have simple frequency characterizations [5]. We extend the concept of Non-Fourier stimuli such as occlusion and translucency from being not explained by its Fourier characteristics to the establishment of exact frequency models of visual stimuli exhibiting occlusions and translucencies.

Non-Fourier motions generate power distributions that are inconsistent with translational motion. Sources of Non-Fourier motion include such phenomena as translucency and occlusion and, in particular, Zanker's Theta motion stimuli involving occlusion [12]. This category of motion is described by an occlusion window that translates with a velocity that is uncorrelated with the velocities of the occluding and occluded signals. For 1D image signals under constant velocity, this type of occlusion scene can be expressed as

$$\begin{aligned} \mathbf{I}(x, t) &= \chi(v_3^{(0)}(x, t))\mathbf{I}_1(v_1^{(0)}(x, t)) \\ &- \chi(v_3^{(0)}(x, t))\mathbf{I}_2(v_2^{(0)}(x, t)) \\ &+ \mathbf{I}_2(v_2^{(0)}(x, t)). \end{aligned} \quad (28)$$

As Zanker and Fleet [12], [5], we model the occlusion win-

dow with a rectangle function in the spatial coordinate as

$$\chi\left(\frac{x-x_0}{b}\right) = \begin{cases} 0 & \text{if } \left|\frac{x-x_0}{b}\right| > \frac{1}{2} \\ \frac{1}{2} & \text{if } \left|\frac{x-x_0}{b}\right| = \frac{1}{2} \\ 1 & \text{if } \left|\frac{x-x_0}{b}\right| < \frac{1}{2}. \end{cases} \quad (29)$$

Such a function has a non-zero value in the interval $[x_0 - \frac{b}{2}, x_0 + \frac{b}{2}]$ and zero otherwise. We then write the Fourier transform of the occlusion scene (28) as

$$\begin{aligned} \mathbf{I}(k, \omega) &= \\ &K \sum_{n=-\infty}^{\infty} \text{sinc}(k - nk_1)c_{1n}\delta(kv_3 - nk_1\Delta a_3) - \\ &K \sum_{n=-\infty}^{\infty} \text{sinc}(k - nk_2)c_{2n}\delta(kv_3 - nk_2\Delta a_2) + \\ &\sum_{n=-\infty}^{\infty} c_{2n}\delta(k - nk_2, \omega + nk_2a_{22}), \end{aligned} \quad (30)$$

where $\text{sinc}(k) = \frac{\sin k}{k}$, $\Delta a_3 = a_{32} - a_{12}$, $\Delta a_2 = a_{22} - a_{12}$ and the phase shift from x_0 in (29) is $K = b^{-1}e^{-ikx_0b^{-1}}$. The spectra $\delta(ka_{32} + \omega - nk_1\Delta a_3)$ and $\delta(ka_{32} + \omega - nk_2\Delta a_2)$ are consonant with the motion of the occluding window and represent a case of Non-Fourier motion, as they do not contain the origin.

We performed two experiments with Theta motions as pictured in Figure 4. It is easily observed that the spectrum of the sinc function is convolved with each frequency of both signals and that its orientation is descriptive of the velocity of the window. As expected, the visible peaks represent the motions of both signals in the usual sense.

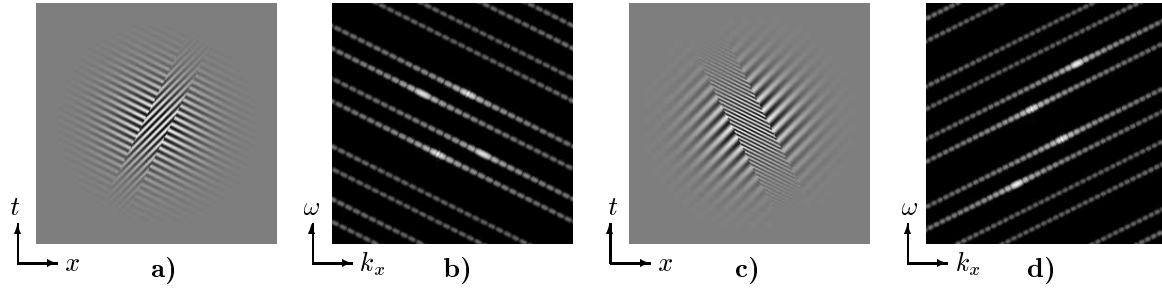


Fig. 4. *Examples of Theta Motion. a):* Velocities of occlusion window, occluding and occluded signals are $a_3 = 0.5$, $v_1 = 1.0$ and $v_2 = -2.0$ respectively. *b):* Frequency spectrum of a). *c):* Velocities of occlusion window, occluding and occluded signals are $v_3 = -0.5$, $v_1 = -2.0$ and $v_2 = 1.0$ respectively. *d):* Frequency spectrum of c).

IV. CONCLUSION

The motivation for such a theoretical framework emanates from the observation that occlusion and translucency in the context of computing optical flow constitute difficult challenges and threatens its precise computation. The theoretical results cast light on the exact structure of occlusion in the frequency domain.

Theorem 1 addresses occlusion in the simplest context and even with such restrictive assumptions, the frequency structure of occlusion can be outlined. Theorem 2 generalizes Theorem 1 to signals composed of an arbitrary number of discrete frequencies. Dirichlet conditions are hypothesized for each signal, since any physical signal satisfies such conditions. It follows that complex exponential expansions are suitable to represent them. The properties of Theorem 1 hold for the arbitrary signals of Theorem 2 as it is possible to measure both velocities and associate them with their respective signal. In addition, Theorems 2 and 3 show that the frequency structure of occlusion is invariant with respect to translational and linear models of signal velocity. It is also shown that the theoretical approach is capable of expressing the frequency structure of non-Fourier motions.

ACKNOWLEDGMENTS

The authors wish to thank NSERC for supporting this research.

REFERENCES

- [1] J. Aisbett. Optical flow with intensity-weighted smoothing. *IEEE PAMI*, 11(5):512–522, 1989.
- [2] C. Chubb and G. Sperling. Drift-balanced random stimuli: A general basis for studying non-fourier motion perception. *J. Opt. Soc. Am. A*, 5(11):1986–2007, 1988.
- [3] D. J. Fleet. *Measurement of Image Velocity*. Kluwer Academic Publishers, Norwell, 1992.
- [4] D. J. Fleet and A. D. Jepson. Computation of component image velocity from local phase information. *IJCV*, 5(1):77–104, 1990.
- [5] D. J. Fleet and K. Langley. Computational analysis of non-fourier motion. *Vision Research*, 34(22):3057–3079, 1995.
- [6] J. D. Gaskill. *Linear Systems, Fourier Transforms and Optics*. Wiley & Sons, Inc., 1978.
- [7] A. D. Jepson and M. Black. Mixture models for optical flow computation. In *IEEE Proceedings of CVPR*, pages 760–761, New York, New York, June 1993.
- [8] H.-H. Nagel. Constraints for the estimation of vector fields from

image sequences. In *Proceedings of IJCAI*, pages 945–951, Karlsruhe, Federal Republic of Germany, August 1983.

- [9] H.-H. Nagel. Displacement vectors derived from second-order intensity variations in image sequences. *CVGIP*, 21:85–117, 1983.
- [10] H.-H. Nagel. On the estimation of optical flow: Relations between different approaches and some new results. *Artificial Intelligence*, 33:299–324, 1987.
- [11] J. D. Victor and M. M. Conte. Coherence and transparency of moving plaids composed of fourier and non-fourier gratings. *Perception & Psychophysics*, 52(4):403–414, 1988.
- [12] M. J. Zanker. Theta motion: A paradoxical stimulus to explore higher-order motion extraction. *Vision Research*, 33:553–569, 1993.